[1] D. D. D. Ma, C. S. Lee, F. C. K. Au, S. Y. Tong, S. T. Lee, *Science* **2003**, *299*, 1874.

[2] a) J. A. Zapien, Y. Jiang, X. M. Meng, W. Chen, F. C. K. Au, Y. Lifshitz, S. T. Lee, *Appl. Phys. Lett.* **2004**, *84*, 1189. b) C. H. Liu, J. A. Zapien, Y. Yao, X. M. Meng, C. S. Lee, S. S. Fan, Y. Lifshitz, S. T. Lee, *Adv. Mater.* **2003**, *15*, 838.

[3] J. C. Johnson, H. Yan, P. Yang, R. J. Saykally, *J. Phys. Chem. B* **2003**, *107*, 8816.

[4] D. Steiner, D. Katz, O. Millo, A. Aharoni, S. H. Kan, T. Mokari, U. Banin, *Nano Lett.* **2004**, *4*, 1073.

[5] H. M. Kim, Y. H. Cho, H. Lee, S. Kim, S. R. Ryu, D. Y. Kim, T. W. Kang, K. S. Chung, *Nano Lett.* **2004**, *4*, 1059.

[6] a) Y. Jiang, X.-M. Meng, J. Liu, Z.-Y. Xie, C.-S. Lee, S. T. Lee, *Adv. Mater.* **2003**, *15*, 323. b) C. Ma, D. Moore, J. Li, Z. L. Wang, *Adv. Mater.* **2003**, *15*, 228.

[7] a) H. Q. Yan, J. C. Johnson, M. Law, R. R. He, K. Knusten, J. R. McKinney, J. Pham, R. Saykally, P. D. Yang, *Adv. Mater.* **2003**, *15*, 1907. b) M. Law, D. J. Sirbuly, J. C. Johnson, J. Goldberger, R. J. Saykally, P. Yang, *Science* **2004**, *305*, 1269.

[8] J. C. Johnson, K. P. Knutsen, H. Q. Yan, M. Law, Y. F. Zhang, P. D. Yang, R. J. Saykally, *Nano Lett.* **2004**, *4*, 197.

[9] Y. K. Liu, C. Y. Geng, J. A. Zapien, Y. Y. Shan, C. S. Lee, Y. Lifshitz, S. T. Lee, *Appl. Phys. Lett.* **2004**, *85*, 3241.

[10] M. Kiihnelt, L. Reindl, E. Griebl, B. Hahn, S. Kaiser, M. Kastnera, H. Preisa, T. Freyb, T. Reisinger, H. P. Wagner, W. Gebhardt, *J. Cryst. Growth* **1998**, *184*, 1165.

[11] X. Duan, Y. Huang, R. Agarwal, C. M. Lieber, *Nature* **2003**, *421*, 24.

[12] H. Kind, H. Yan, B. Messer, M. Law, P. D. Yang, *Adv. Mater.* **2002**, *14*, 158.

[13] I. Suemune, *J. Appl. Phys.* **1990**, *67*, 2364.

[14] M. W. Wang, J. O. McCaldin, J. F. Swenberg, T. C. McGill, R. J. Hauenstein, *Appl. Phys. Lett.* **1995**, *66*, 1974.

[15] J. Ding, T. Lshihara, M. Hagerott, H. Jeon, A. V. Nurmikko, *Phys. Rev. B: Condens. Matter Mater. Phys.* **1993**, *47*, 10 528.

[16] R. Cingolani, R. Rinaldi, L. Calcagnile, P. Prete, P. Sciacovelli, L. Tapfer, L. Vanzetti, G. Mula, F. Bassani, L. Sorba, A. Franciosi, *Phys. Rev. B: Condens. Matter Mater. Phys.* **1994**, *49*, 16 769.

[17] E. Kato, H. Noguchi, M. Nagai, H. Okuyama, S. Kijima, A. Ishibashi, *Electron. Lett.* **1998**, *34*, 282.

[18] S. Fuke, C. Maezawa, K. Nakamura, K. Kuwahara, *J. Appl. Phys.* **1992**, *71*, 3611.

[19] H. Oniyama, S. Yarnaga, A. Yoshikawa, *Jpn. J. Appl. Phys., Part 2* **1989**, *28*, L2137.

[20] R. Dahmani, L. Salamanca-Riba, N. Y. Ngugen, D. Chandler-Horowitz, B. T. Jonker, *J. Appl. Phys.* **1994**, *76*, 514.

[21] S. Z. Fujita, T. Asano, K. Maehara, S. G. Fujita, *Appl. Surf. Sci.* **1994**, *79–80*, 270.

[22] T. Yokogawa, T. Ishikawa, J. L. Merz, T. Taguchi, *J. Appl. Phys* **1994**, *75*, 2189.

[23] J. M. Dona, J. Herrero, *J. Electrochem. Soc.* **1997**, *144*, 4091.

[24] T. Mahalingam, C. Sanjeeviraja, *Phys. Status Solidi A* **1992**, *129*, K89.

[25] P. Cherlin, E. L. Lind, E. A. Davis, *J. Electrochem. Soc.* **1970**, *117*, 233.

[26] D. W. G. Ballentyne, B. Ray, *Physica* **1961**, *27*, 337.

[27] G. Shimaoka, Y. Suzuki, *Appl. Surf. Sci.* **1997**, *113*, 528.

[28] Y. W. Wang, L. D. Zhang, C. H. Liang, G. Z. Wang, X. S. Peng, *Chem. Phys. Lett.* **2002**, *357*, 314.

[29] Y. C. Zhu, Y. Bando, D. F. Xue, *Appl. Phys. Lett.* **2003**, *82*, 1769.

[30] D. Denzler, M. Olschewski, K. Sattler, *J. Appl. Phys.* **1998**, *84*, 2841.

[31] A. M. Salem, *Appl. Phys. A: Mater. Sci. Process.* **2002**, *74*, 205.

[32] A. Abounadi, M. Di Blasio, D. Bouchara, J. Calas, M. Averous, O. Briot, N. Briot, T. Cloitre, R. L. Aulombard, B. Gil, *Phys. Rev. B: Condens. Matter Mater. Phys.* **1994**, *50*, 11 677.

[33] M. Fernández, P. Prete, N. Lovergine, A. M. Mancini, R. Cingolani, L. Vasanelli, M. R. Perrone, *Phys. Rev. B: Condens. Matter Mater. Phys.* **1997**, *55*, 7660.

[34] a) B. Mroziewicz, M. Bugajski, W. Nakmaski, *Physics of Semiconductor Lasers*, Elsevier, Amsterdam **1991**. b) K. Iga, *Fundamentals of Laser Optics*, Plenum, New York **1994**.


# Extraordinary Strengthening Effect of Carbon Nanotubes in Metal-Matrix Nanocomposites Processed by Molecular-Level Mixing**

By *Seung I. Cha*, *Kyung T. Kim*, *Salman N. Arshad*, *Chan B. Mo*, and *Soon H. Hong**

Since the first discovery of carbon nanotubes (CNTs) in 1991, a window to new technological areas has been opened.[1] One of the emerging applications of CNTs is the reinforcement of composite materials to overcome the performance limits of conventional materials.[2,3] Recent developments in CNT/polymer composites have shown the potential for improving the strength of polymers,[2] and this finding has encouraged researchers to use carbon nanotubes as reinforcements for metal and ceramic matrices.[4–7] However, because of the difficulties in distributing CNTs homogeneously in a metal or ceramic matrix by means of traditional composite processes, it has been doubted whether CNTs can really reinforce metals or ceramics.[4–7] Here we report on a CNT-reinforced Cu matrix nanocomposite, fabricated by a novel fabrication process called "molecular-level mixing"; this nanocomposite shows extremely high strength, several times higher than the matrix. The novel process for fabricating CNT/Cu composite powders involves suspending CNTs in a solvent by surface functionalization, mixing Cu ions with the CNT suspension, drying, calcination, and reduction. This process produces CNT/Cu composite powders, whereby the CNTs are homogeneously implanted within the Cu powders. The CNT/Cu nanocomposite, consolidated by spark plasma sintering of CNT/Cu composite powders, is shown to possess three times the strength of the Cu matrix and to have twice the Young's modulus. This extraordinary strengthening effect of carbon nanotubes in metal is higher than that of any other reinforcement ever used for metal-matrix composites.

Several researchers have attempted to fabricate CNT-reinforced metal- or ceramic-matrix composite materials by

[*] Prof. S. H. Hong, Dr. S. I. Cha, K. T. Kim, S. N. Arshad, C. B. Mo
Department of Materials Science and Engineering
Korea Advanced Institute of Science and Technology
373-1 Kusong-Dong, Yusong-Gu, Daejeon 305-701 (Korea)
E-mail: shhong@kaist.ac.kr

[**] This research was supported by a grant (Code No. 05K1501-00510) from the "Center for Nanostructured Materials Technology" under the "21st Century Frontier R&D Programs" of the Ministry of Science and Technology, Korea. Supporting Information is available online from Wiley InterScience or from the author.

 DOI: 10.1002/adma.200401933  

ADVANCED MATERIALS

means of traditional powder-metallurgy processes,[4,6,7] which consist of mixing CNTs with matrix powders followed by sintering or hot-pressing. However, these attempts have failed to fabricate CNT/metal or CNT/ceramic composites with homogeneously dispersed CNTs in the matrix. This is mainly due to the strong agglomeration of CNTs in the powder form: the van der Waals' forces between CNTs cause them to mutually attract each other rather than homogeneously disperse. Furthermore, if the CNT/metal or CNT/ceramic nanocomposites are manufactured by conventional processes, most of the CNTs are located on the surfaces of the metal or ceramic powders after mixing.[4,6,7] The conventional process inhibits the diffusion of matrix materials across or along the powder surfaces; hence, sintering cannot proceed without damaging the CNTs or removing them from the powder surfaces. Even if sintering is successful, CNTs are mostly located at grain boundaries of the matrix and are insignificant in improving material performance. At the same time, the most important processing issue is the interfacial strength between the carbon nanotubes and the matrix. In the case of CNT/polymer nanocomposites, the interfacial strength between the CNTs and the polymer matrix is strong because they interact at the molecular level.[2] In the case of CNT/metal or CNT/ceramic nanocomposites, however, the interfacial strength cannot be expected to be high because the CNTs and the matrix are merely blended.[4]

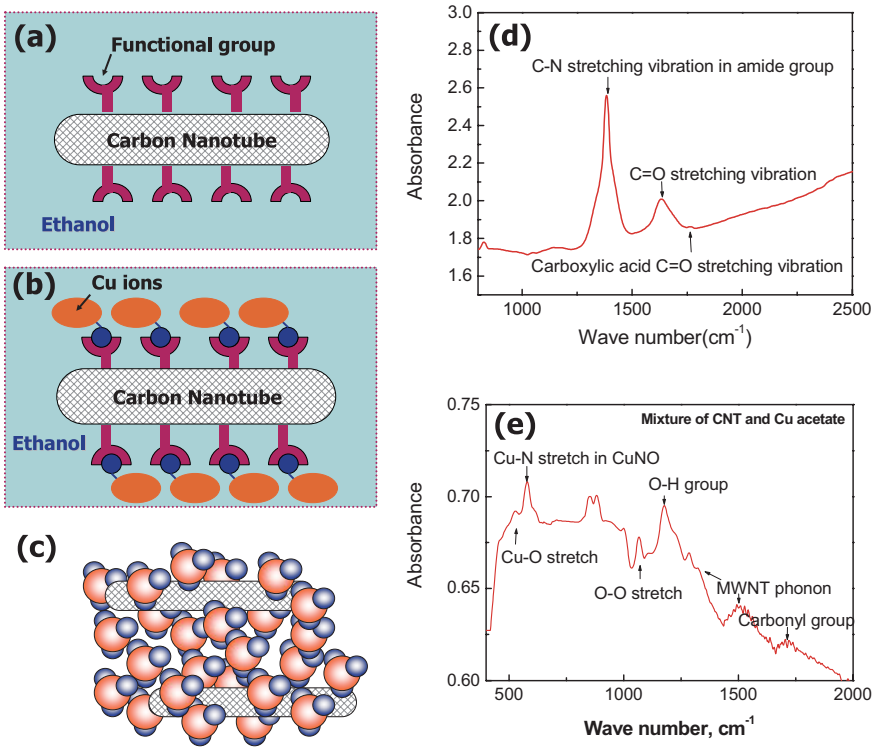


**Figure 1.** Schematics depicting strategies and procedures for the molecular-level mixing process to fabricate CNT/Cu composite powders: a) making a functionalized stable CNT suspension in ethanol, b) dissolution of a Cu salt such as $Cu(CH_3COO)_2$ and attaching Cu ions to the functional groups on the surface of the CNT, c) vaporization of the solvent by heating. d) Fourier-transform IR (FTIR) spectroscopic analysis of CNTs after purification, which shows that some functional groups containing N and O formed on the surface of the CNTs, and e) FTIR analysis of dried powders before calcination, which shows that Cu ions reacted with the functional groups on the CNTs. (MWNT: multiwalled nanotube.)

Our strategy for developing a novel fabrication process for CNT/Cu nanocomposites basically involves molecular-level mixing of the reinforcement (CNT) and the matrix material in a solution instead of conventional powder mixing. This new process produces CNT/Cu composite powders, where the CNTs are mainly located within the Cu powders rather than on their surfaces; the chemical bonding between the CNTs and the Cu ions provides a homogeneous distribution of CNTs, as well as high interfacial strength between the CNTs and Cu.

The suggested process for fabricating CNT/Cu composite powders consists of four steps. First, CNT powders produced by thermal chemical vapor deposition are dispersed in a solution such as water or ethanol to make a stable suspension by attaching functional groups onto the CNT surfaces (Figs. 1a,d). There are several chemical methods for attaching functional groups to CNT surfaces.[8–11] Once the functional groups are attached to the CNTs, the electrostatic repulsive force between the CNTs overcomes the van der Waals' force to form a stable suspension within the solvent. Second, a salt containing Cu ions—copper acetate in the current study—is dissolved in the CNT suspension. The solution now consists of suspended CNTs, solvent, ligands, and metal ions. Additional sonication treatment assists the dispersion of Cu ions among the suspended CNTs and promotes the reaction between the Cu ions and the functional groups on CNT surfaces (Figs. 1b,e). The third step is to dry the solution by heating at 100–250 °C in air. During this process, the solvent and ligands are removed and the Cu ions on the CNTs are oxidized to form powders (Fig. 1c). The fourth and final step is the calcination and reduction process to obtain chemically stable crystalline powders. The powders obtained in the third step are generally a mixture of CuO and $Cu_2O$. These powders are changed into stable CNT/CuO by heating at 300 °C in air and are then reduced to CNT/Cu composite powders by a reduction process under a hydrogen atmosphere.

The above four-step process gave homogeneously dispersed CNTs within Cu powders, as shown in Figure 2. The most important feature of this process is that CNTs and Cu ions are mixed with each other at the molecular level. That is, the

  

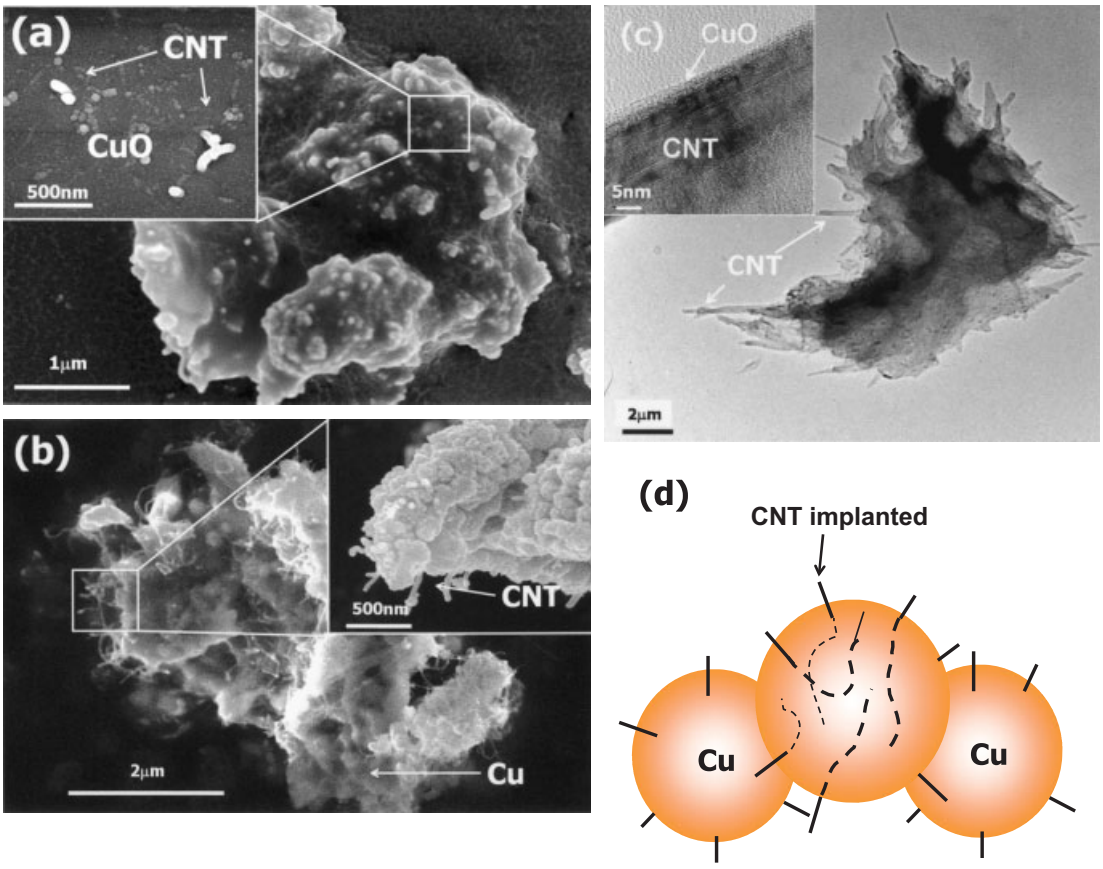


**Figure 2.** Microstructures of CNT/CuO and CNT/Cu composite powders, where the CNTs are homogeneously implanted in the matrix. a) Scanning electron microscopy (SEM) micrographs of CNT/CuO composite powders, b) SEM micrographs of CNT/Cu composite powders, c) transmission electron microscopy (TEM) micrographs of CNT/CuO composite powders, showing that CNTs are implanted within the matrix with good bonding at the interface between CuO and the CNTs (inset), and d) schematic depiction of the CNT/Cu composite powder.

CNTs are located within the powders rather than on the powder surfaces. The morphologies of the CNT/CuO and CNT/Cu powders show an ideal composite microstructure, which displays spherical morphologies with CNTs implanted in the powders (Figs. 2a,b). The implanted CNTs in the CNT/Cu composite powders could be seen more clearly using transmission electron microscopy (TEM, Fig. 2c). The finally obtained CNT/Cu composite powder, wherein CNTs are implanted in the Cu matrix, is schematically depicted in Figure 2d.

The CNT/Cu composite powders fabricated by the molecular-level mixing process were consolidated into a bulk CNT/Cu nanocomposite with full densification by spark plasma sintering, which can produce a high heating rate of 100 °C min$^{-1}$ and rapid consolidation through high-joule heating and a spark plasma generated between the powders. A schematic depiction of the spark plasma sintering process and the microstructure of the resulting CNT/Cu nanocomposites is shown in Figure 3a. The consolidated CNT/Cu nanocomposite shows a homogeneous distribution of carbon nanotubes within the Cu matrix, which had not been obtained until now for CNT/metal or CNT/ceramic nanocomposites (Fig. 3b). Particularly, the TEM micrograph (Fig. 3c) shows that the carbon nanotubes form a network within the Cu grains. Moreover, the Cu grains show a very low dislocation density when they are reinforced by carbon nanotubes.

The mechanical properties of the CNT/Cu nanocomposite were characterized using compressive tests. As shown in Figure 4a, the compressive yield strengths of CNT/Cu nanocomposites were much higher than that of the Cu matrix, which was fabricated by the same process without adding CNTs. A 5 vol.-% CNT-reinforced Cu matrix nanocomposite showed a yield strength of 360 MPa, which is 2.3 times higher than that of Cu. In the case of 10 vol.-% CNT-reinforced Cu, the yield strength was 455 MPa, which is more than 3 times higher than that of Cu. Moreover, the Young's modulus of the CNT/Cu nanocomposite increased as the volume fraction of carbon nanotubes was increased, as shown in Figure 4b.

Such remarkable strengthening by CNT reinforcement was due to the high load-transfer efficiency of CNTs in the metal matrix. High load-transfer efficiency was caused by strong interfacial strength between CNTs and Cu, which originated from chemical bonds formed during the molecular-level mix-

  

ADVANCED MATERIALS

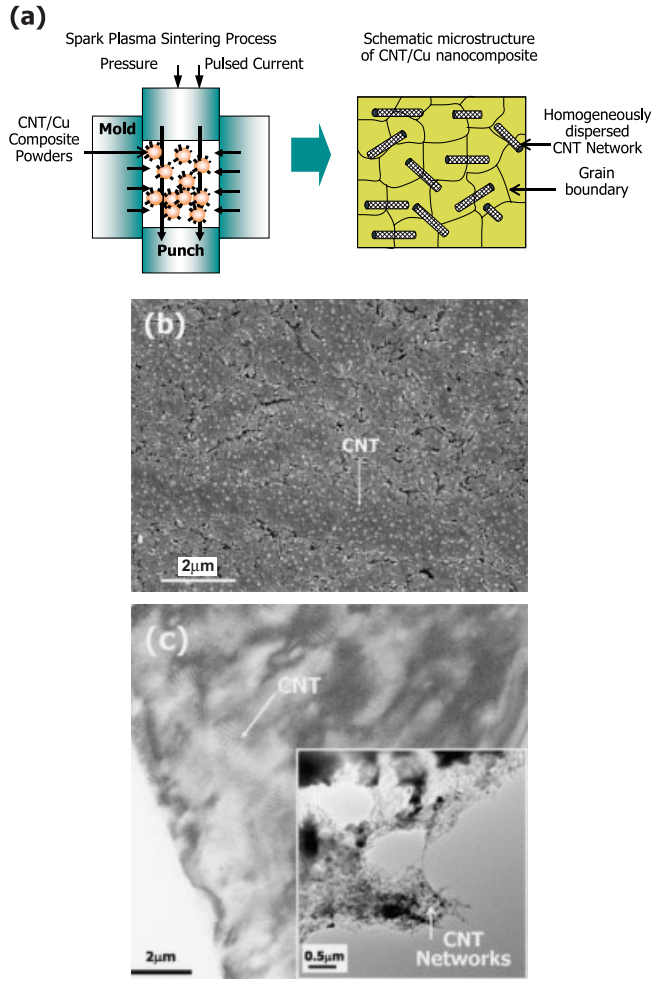


**Figure 3.** a) Schematic of the spark plasma sintering process and the resulting microstructure of the CNT/Cu nanocomposite. b) SEM micrographs showing homogeneous distribution of CNTs in the CNT/Cu nanocomposite with 5 vol.-% of CNTs, as revealed after chemical etching. c) TEM micrographs showing a three-dimensional network of CNTs in the Cu grains.

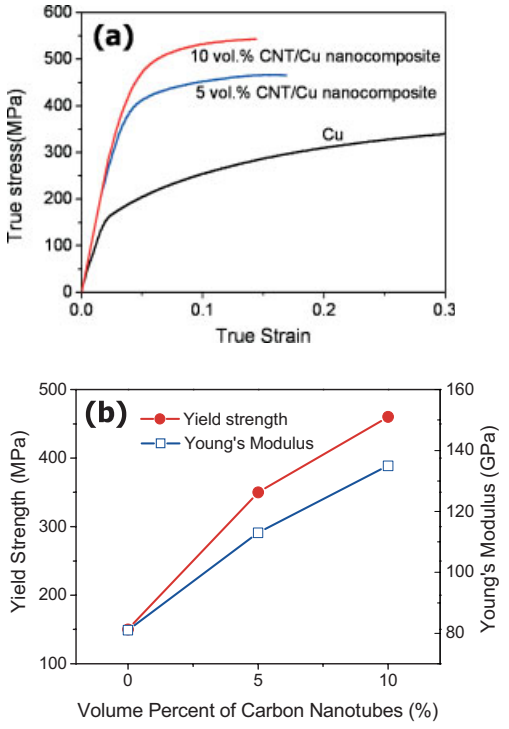


**Figure 4.** Mechanical properties of CNT/Cu nanocomposites: a) stress–strain curves of CNT/Cu nanocomposites obtained by compressive testing, and b) yield strength and Young's modulus of CNT/Cu nanocomposites with increasing volume percentage of CNTs.

ing process. The yield strength of the metal-matrix composites can be expressed as

$$\sigma = \sigma_m(1 + V_f R) \quad (1)$$

where $R$ is the strengthening efficiency of reinforcement, $V_f$ is the volume fraction of reinforcement, and $\sigma_m$ is the yield strength of the matrix.[12] Using the generalized shear-lag model, the strengthening efficiency $R$ can be expressed as $S/2$, where $S$ is the aspect ratio of reinforcement, i.e., the ratio between the diameter and length of reinforcement.[12] Using this theory, the calculated yield strengths of 5 vol.-% and 10 vol.-% CNT reinforced Cu matrix composites are 370 MPa and 589 MPa, respectively. These values are higher than those measured by the compressive test. This disparity is derived mainly from the misalignment of the carbon nanotubes within the Cu matrix.[12] The above equation is based on the perfect alignment of fibrous reinforcement in the loading direction. In the CNT/Cu nanocomposite, however, the carbon nanotubes form a three-dimensional network within the Cu matrix, and as a result the load-transfer efficiency decreases. It must be noted that strengthening by reinforcement is separate from other strengthening mechanisms, including precipitation strengthening, grain-refinement strengthening, and work hardening. Therefore, if the strength of the Cu matrix reaches 1 GPa using other strengthening mechanisms, such as nanostructuring of grain size, the strength of the CNT/Cu nanocomposite can be enhanced over 3 GPa by strengthening of the CNTs. Nonetheless, the strengthening effect of CNT reinforcement is the greatest of all reinforcements used for metal matrix composites. As shown in Table 1, the reinforcement efficiency, i.e., the strengthening effect of a given volume percentage of reinforcement on the matrix, is almost eight times higher for carbon nanotubes than for SiC particles and three times higher than for SiC whiskers, which are the two most widely used strengthening reinforcements for metal matrices. This indicates that carbon nanotubes are confirmed to be the most effective reinforcements.

Lastly, it is worth mentioning here that the molecular-level mixing process described above can also be applied to CNT/ceramic nanocomposites by omitting the reduction step. As shown in the Supporting Information, CNT/alumina nanocomposites can be fabricated by using $Al(NO_3)_3 \cdot 9H_2O$. Here, as in the case of the CNT/Cu nanocomposite, CNTs were

  

**Table 1.** Strengthening efficiencies of several reinforcement materials. The strengthening efficiency of reinforcement *R* is defined as the ratio of the amount of yield strength increase of the composite to that of the matrix by the addition of reinforcement materials [13–18].

| Reinforcement | | Matrix | | Composite | Strengthening efficiency of reinforcement *R* [a] |
|---|---|---|---|---|---|
| Type | Vol. [%] | Type | Yield strength $\sigma_m$ [MPa] | Yield strength $\sigma_c$ [MPa] | |
| Alumina Particle | 10 | Zn/Al/Cu | 310 | 380 | 2.3 |
| Alumina Fiber | 10 | Al/12Si/Ni/Cu | 210 | 247 | 1.7 |
| SiC Particle | 10 | Al alloy CW67 | 340 | 425 | 2.5 |
| SiC Whisker | 10 | Al alloy AZ91 | 87 | 154 | 7.6 |
| Carbon Fiber | 10 | Al alloy A357 | 360 [b] | 499 [b] | 3.9 |
| Carbon Fiber | 10 | Cu | 232 [b] | 347 [b] | 5.0 |
| Carbon Nanotube | 10 | Cu | 150 | 455 | 20.3 |

[a] Strengthening efficiency of reinforcement $R = (\sigma_c - \sigma_m)/V_f \sigma_m$.
[b] The strength of the carbon-fiber-reinforced composite is fracture stress.

implanted within the alumina matrix, and the CNT/alumina nanocomposite showed much-improved strength and fracture toughness.

In summary, CNT/Cu nanocomposites with homogeneously dispersed CNTs within the Cu matrix can be fabricated by means of a molecular-level mixing process, which consists of mixing Cu ions with functionalized CNTs in a solvent. The yield strength of the CNT/Cu nanocomposite was shown to be three times higher than that of Cu alone. Carbon nanotubes showed the most effective strengthening efficiencies among all reinforcement materials: eight times higher than SiC particles and three times higher than SiC whiskers.

## *Experimental*

*Fabrication of CNT/Cu Composite Powders*: Multiwalled carbon nanotubes, with diameters of 10–40 nm and fabricated by thermal chemical vapor deposition, were purified and functionalized by acid treatment using HF, $H_2SO_4$, and $HNO_3$. The CNTs were stirred for 24 h in HF and then cleansed with a mixed solution of $H_2SO_4/HNO_3$ in a 3:1 ratio. 20 mg of the purified CNTs was dispersed in 500 mL ethanol by sonication for 2 h to form a stable suspension. 3 g of $Cu(CH_3COO)_2{\cdot}H_2O$ (Aldrich) was added to the CNT suspension, which was sonicated again for 2 h. The solution was vaporized with magnetic stirring at 100 °C, and the dried powders were calcinated at 300 °C in air. The calcinated powders were reduced at 250 °C for 3 h under a hydrogen atmosphere. The average number of walls in the multiwalled carbon nanotubes was measured to be 20 by TEM observations. The density of multiwalled carbon nanotubes with an average diameter of 40 nm and average length of 2 μm was calculated to be 1.8 g cm$^{-3}$. The weight percent of CNTs was 1.0 for the 5 vol.-% CNT/Cu nanocomposite and 2.2 for the 10 vol.-% CNT/Cu nanocomposite.

*Consolidation of CNT/Cu Composite Powders*: The CNT/Cu composite powders were pre-compacted in a graphite mold, 15 mm in diameter, under a pressure of 10 MPa. The pre-compacted powders were consolidated by spark plasma sintering at 550 °C for 1 min in a vacuum of 0.1 Pa with an applied pressure of 50 MPa. The heating rate up to the sintering temperature was maintained at 100 °C min$^{-1}$. The final size of the spark plasma sintered CNT/Cu nanocomposite was 15 mm in diameter and 5 mm in thickness.

*Characterization*: Microstructure characterization of the CNT/Cu composite powders and nanocomposites were carried out using optical microscopy, high-resolution scanning electron microscopy (HRSEM), and TEM. The volume fraction of CNTs was determined by analyzing the carbon contents using an elemental analyzer (Fisons EA1110) and a C/S analyzer (ELTRA CS800). Compressive tests were performed using an Instron 5583 with a crosshead speed of 0.2 mm min$^{-1}$. The sample had a cylindrical disc shape, and was 2 mm in height and 1.5 mm in diameter.

Received: November 26, 2004
Final version: March 7, 2005

[1] R. H. Baughman, A. A. Zakhidov, W. A. de Heer, *Science* **2002**, *297*, 787.
[2] A. A. Mamedov, N. A. Kotov, M. Prato, D. M. Guldi, J. P. Wicksted, A. Hirsch, *Nat. Mater.* **2002**, *1*, 190.
[3] E. T. Thostenson, Z. Ren, T.-W. Chou, *Compos. Sci. Technol.* **2001**, *61*, 1899.
[4] G.-D. Zhan, J. D. Kuntz, J. Wan, A. K. Mukherjee, *Nat. Mater.* **2003**, *2*, 38.
[5] A. Peigney, *Nat. Mater.* **2003**, *2*, 15.
[6] E. Flahaut, A. Peigney, Ch. Laurent, Ch. Marliere, F. Chastel, A. Rousset, *Acta Mater.* **2000**, *48*, 3803.
[7] X. Wang, N. P. Padture, H. Tanaka, *Nat. Mater.* **2004**, *3*, 539.
[8] J. Liu, A. G. Rinzler, H. Dai, J. H. Hafner, R. K. Bradley, P. J. Boul, A. Lu, T. Iverson, K. Shelimov, C. B. Huffman, F. Rodriguez-Macias, Y.-S. Shon, T. R. Lee, D. T. Colbert, R. E. Smalley, *Science* **1998**, *280*, 1253.
[9] M. A. Hamon, J. Chen, H. Hu, Y. Chen, M. E. Itkis, A. P. Rao, P. C. Eklund, R. C. Haddon, *Adv. Mater.* **1999**, *11*, 834.
[10] R. Bandyopadhyaya, E. Nativ-Roth, O. Regev, R. Yerushalmi-Rozen, *Nano Lett.* **2002**, *2*, 25.
[11] W. Huang, Y. Lin, S. Taylor, J. Gaillard, A. M. Rao, Y.-P. Sun, *Nano Lett.* **2002**, *2*, 231.
[12] H. J. Ryu, S. I. Cha, S. H. Hong, *J. Mater. Res.* **2003**, *18*, 2851.
[13] E. Martinez-Flores, J. Negrete, G. T. Villasenor, *Mater. Des.* **2003**, *24*, 281.
[14] M. A. Taha, *Mater. Des.* **2001**, *22*, 431.
[15] D. B. Zaklina, M. Mirjana, *Mater. Charact.* **2001**, *47*, 129.
[16] Z. Minggyi, W. Kun, Y. Congkai, *Mater. Sci. Eng., A* **2001**, *318*, 50.
[17] M. H. Vidal-Setif, M. Lancin, C. Marhic, R. Valle, J.-L. Raviart, J.-C. Daux, M. Rabinovitvch, *Mater. Sci. Eng., A* **1999**, *272*, 321.
[18] Y. Z. Wan, Y. L. Wang, H. L. Luo, X. H. Dong, G. X. Cheng, *Mater. Sci. Eng., A* **2000**, *288*, 26.

  